Microstructure dependence of heat sink constructed by carbon nanotubes for chip cooling

Zhenlong Huang, Min Gao, TaiSong Pan, Yin Zhang, Bo Zeng, Weizheng Liang, Feiyi Liao, and Yuan Lin

Citation: Journal of Applied Physics **117**, 024901 (2015); doi: 10.1063/1.4905589
View online: http://dx.doi.org/10.1063/1.4905589
View Table of Contents: http://scitation.aip.org/content/aip/journal/jap/117/2?ver=pdfcov
Published by the AIP Publishing

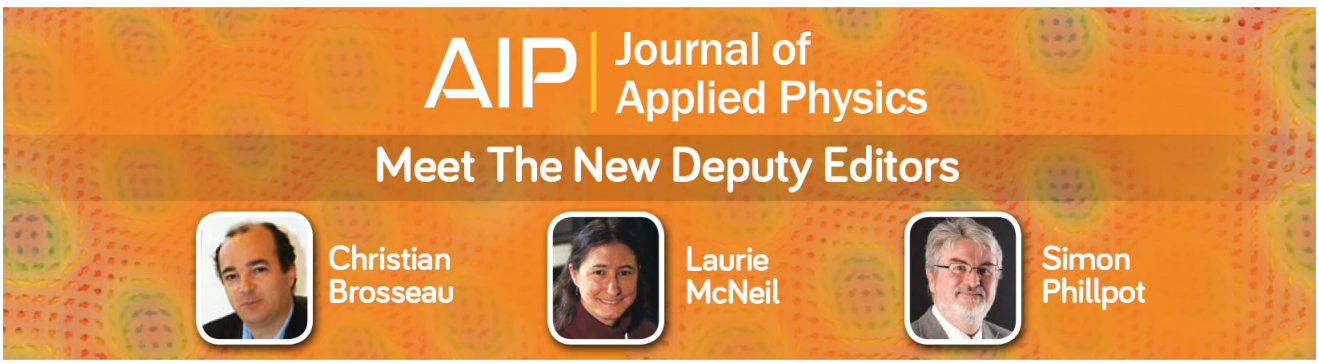

Microstructure dependence of heat sink constructed by carbon nanotubes for chip cooling

Zhenlong Huang,[1] Min Gao,[1,a)] TaiSong Pan,[1] Yin Zhang,[1] Bo Zeng,[1] Weizheng Liang,[1] Feiyi Liao,[1] and Yuan Lin[1,2,a)]
[1]*State Key Laboratory of Electronic Thin films and Integrated Devices, University of Electronic Science and Technology of China, Chengdu, Sichuan 610054, China*
[2]*Institute of Electronic and Information Engineering in Dongguan, University of Electronic Science and Technology of China, Dongguan, 523808 Guangdong, China*

(Received 22 September 2014; accepted 26 December 2014; published online 8 January 2015)

Carbon nanotube (CNT) arrays with aligned growth orientation and sponge CNTs which consist of flocculent carbon fibers with tiny CNTs on their surface were synthesized by chemical vapor deposition. Heat sinks based on CNT arrays or sponge CNTs were made to investigate their heat dissipation performance. It is found that their microstructures have strong impacts on the thermal performance by changing the coefficient of air convection. The long CNT arrays have good heat dissipation performance even under natural convection for its aligned structure and large contacting area with the air, while the sponge CNTs show larger improvement in heat dissipation ability under airflow due to their porous structure. The results give a good reference for developing low-cost, light-weight, and high-performance CNT-based heat sinks for chip cooling under different working conditions. © *2015 AIP Publishing LLC*. [http://dx.doi.org/10.1063/1.4905589]

I. INTRODUCTION

With the development of technology, integrated density of circuits increases quickly, which means more heat will be produced in the same size. Then heat dissipation becomes one of the most serious limitations for a high density integrated device. To get a low-cost and high-performance heat dissipation solution, intensive studies have been conducted on the materials having high thermal conductivity as well as large contact area with air.[1–3] Carbon nanotubes (CNTs), with its high thermal conductivity[4,5] and large specific surface area,[6,7] are a potential candidate for the thermal management. Thus, the heat sink based on CNTs has been purposed.[8–10] Although many results have been reported on the modification of CNT type, including CNT arrays,[11] patterned CNTs,[12] and buckypaper,[13] there has been few research result involving the relationship of heat performance between micro structures of CNTs and their air convection efficiency.

In this paper, we used sponge CNTs and CNT arrays to test and discuss the heat dissipation of CNTs with different microstructures. Here, the sponge CNT refers to one of the carbon structures we synthesized which has flocculent major branches with diameter of micrometer-size and tiny branches of nanometer-size grown on the surface of the main branches. It is a sponge-like bulk material with light-weight, high porosity, and large surface area. It can be forced into any required shape without damage,[14] which is very important for a stable assembly of a heat sink. A unique test structure is designed to simulate the practical thermal environment of microelectronic devices. By using this test structure, the thermal dissipation performance of long CNT arrays, short CNT arrays, and sponge CNTs were studied, respectively. Our results show that CNTs with more interspace and surface area have a better thermal dissipation performance with a higher coefficient of air convection.

II. EXPERIMENTAL

The floating catalyst chemical vapor deposition (CVD) method was used to synthesize CNT arrays and sponge CNTs.[15–18] Precursor solution was introduced in the quartz tube of a furnace by an injector. A Si substrate with a 300-nm-thick SiO_2 layer was put in the middle of the quartz tube as a holder. Then the quartz tube was heated to the growth temperature under the protection of argon. Precursor solution in a carrier gas was preheated to 200 °C at the first preheating stage with an injection speed of 8 mL/h. By controlling the concentration of precursor solution and growth condition, different types of CNTs can be obtained. In this study, two conditions were used: (1) for sponge CNTs, the precursor solution is 2 wt. % ferrocene in cyclohexane, and the growth temperature is 900 °C, the carrier gas is argon only; (2) for CNT arrays, the precursor solution is 2 wt. % ferrocene in dimethylbenzene, the growth temperature is 800 °C, and the carrier gas is 10% H_2 in argon. CNT arrays with different length can be prepared by varying the growth time.

The micro structures of different CNTs are shown in Fig. 1. CNTs in the CNT arrays have the same growth orientation and stand one by one, as shown in Fig. 1(a). The diameter of the CNTs is about 15 nm and the specific surface area is about 125 m^2/g based on the data from Ref. 7. On the other hand, as shown in Figs. 1(b) and 1(c), sponge CNTs have flocculent major branches with large diameter (about 2.86 μm) and tiny branches grown on the surface of the main branches. The diameter of the tiny branches is about 104 nm and the length is about 1 μm. In consideration of the diameter and the material shape, the major branches should be carbon

a)Authors to whom correspondence should be addressed. Electronic addresses: mingao@uestc.edu.cn and linyuan@uestc.edu.cn

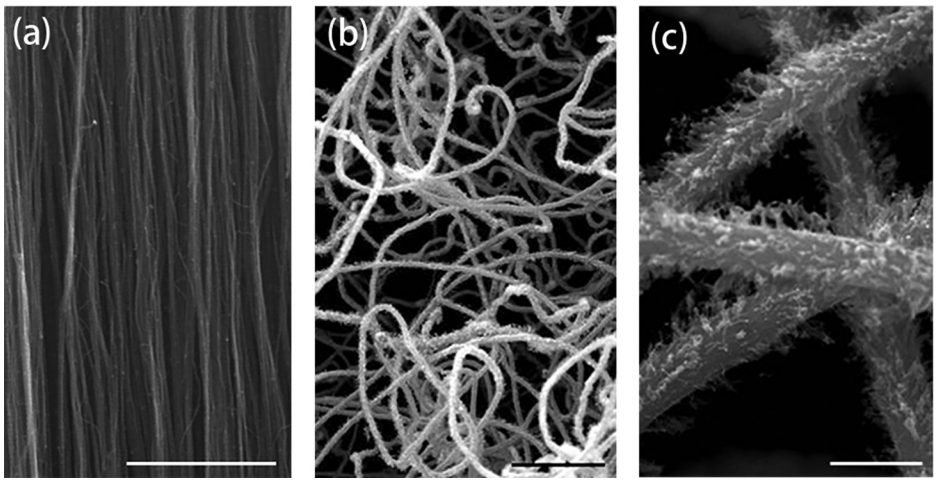

FIG. 1. Morphology of carbon nanotubes. (a) SEM image of the CNT arrays (scale bar: 1 μm). (b) SEM image of the sponge CNTs (scale bar: 50 μm). (c) Zoom-in SEM image of sponge CNTs (scale bar: 5 μm). Some tiny branches (CNTs) grow on the surface of major branches (carbon fiber).

fiber and the tiny branches are multiwalled CNTs. The specific surface area of the sponge CNTs is about 2.34 m^2/g based on our calculation and the interspaces among the sponge CNTs are bigger than the arrays. Nevertheless, the sponge-like structure makes the CNTs interconnected. Due to the interconnected structure, the sponge CNTs are not easy to disperse, which means the heat sink made of sponge CNTs will be more stable.

To study the thermal dissipation performance of CNT based heat sinks, a dual-side structure on silicon substrate is designed to simulate the thermal environment of microelectronic device. The schematic of the structure is shown in Fig. 2. A heating electrode was made on one side of the silicon substrate and it can be treated as a silicon device chip. Then, silver paste was dropped on the other side of the silicon chip and CNTs were forced onto the silicon with the silver paste. To make silver paste solidify and ensure the good thermal contact between CNTs and silicon chips, we heated the chips on 120 °C for 20 min. At last, in order to better evaluate the performance of the heat sink structure, we used polyvinyl chloride (PVC) to carefully cover the side with heating electrodes, which would minimize the heat dissipation from this side. Three kinds of samples had been made in the structure as shown in Fig. 2. The difference among these three is the microstructure or length of CNTs. These three kinds of CNTs are long CNT arrays with length of 2000 μm, short CNT arrays with length of 500 μm, and sponge CNTs with length of 2000 μm. Besides, a sample without any CNTs was used as a reference. All the tests were conducted

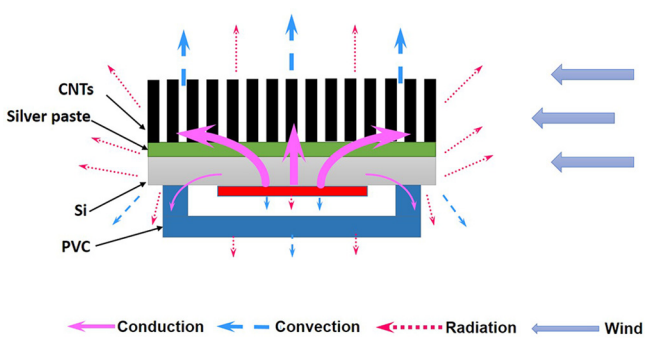

FIG. 2. The schematic of the test structure.

at room temperature (25 °C). The temperature coefficient of heating electrode was determined first by monitoring its resistance at different temperatures and the results are shown in Fig. 3(a). So, the temperature of the electrodes can be calculated by measuring the resistance of itself. In other words, the heating electrodes serve as thermometer as well. To evaluate the thermal performance of the test chips, a constant current was applied on the electrode, then the real-time changes of the resistance can be obtained by standard four probe method, which can be converted into the temperature of the electrodes (similar to the junction temperature in a real device). Thus, the dissipation ability of the heat sinks can be reflected by comparing the temperature of the electrodes. By varying the applied electric currents and the external wind speeds, we performed a systematic study to establish the relationship between balanced electrode temperature, power density, and cross-ventilation. The current through the heating electrode was varied from 30 mA to 100 mA. The wind forced on the samples was from 0 m/s to 2.0 m/s.

III. RESULTS AND DISCUSSION

Fig. 3(b) shows the changes of electrode temperature with time when a 100 mA current was applied on the chip with short CNT arrays heat sink, in the circumstance with different wind speeds. The temperature rises once a current passes the electrode and it tends to be balanced after a period of time. Obviously, when the wind speed increases, it needs a shorter time to get balanced and a lower balanced temperature is obtained. Similar trend was observed in the other three kinds of samples. The correlation between the temperature increase and time indicates that two stages of heat dissipation, unsteady process and steady process, were involved. At the initial stage, the heat generated by electric current caused a temperature rise. Then, as the result of heat transfer, the system gradually becomes equilibrium and the temperature keeps steady when the balance between heat generation and heat dissipation can be achieved.

At the unsteady stage, the heat produced by the heating electrodes was mainly conducted to the heat sink side and then dissipated to air. The temperature change with time at the unsteady stage can be described by following equations:

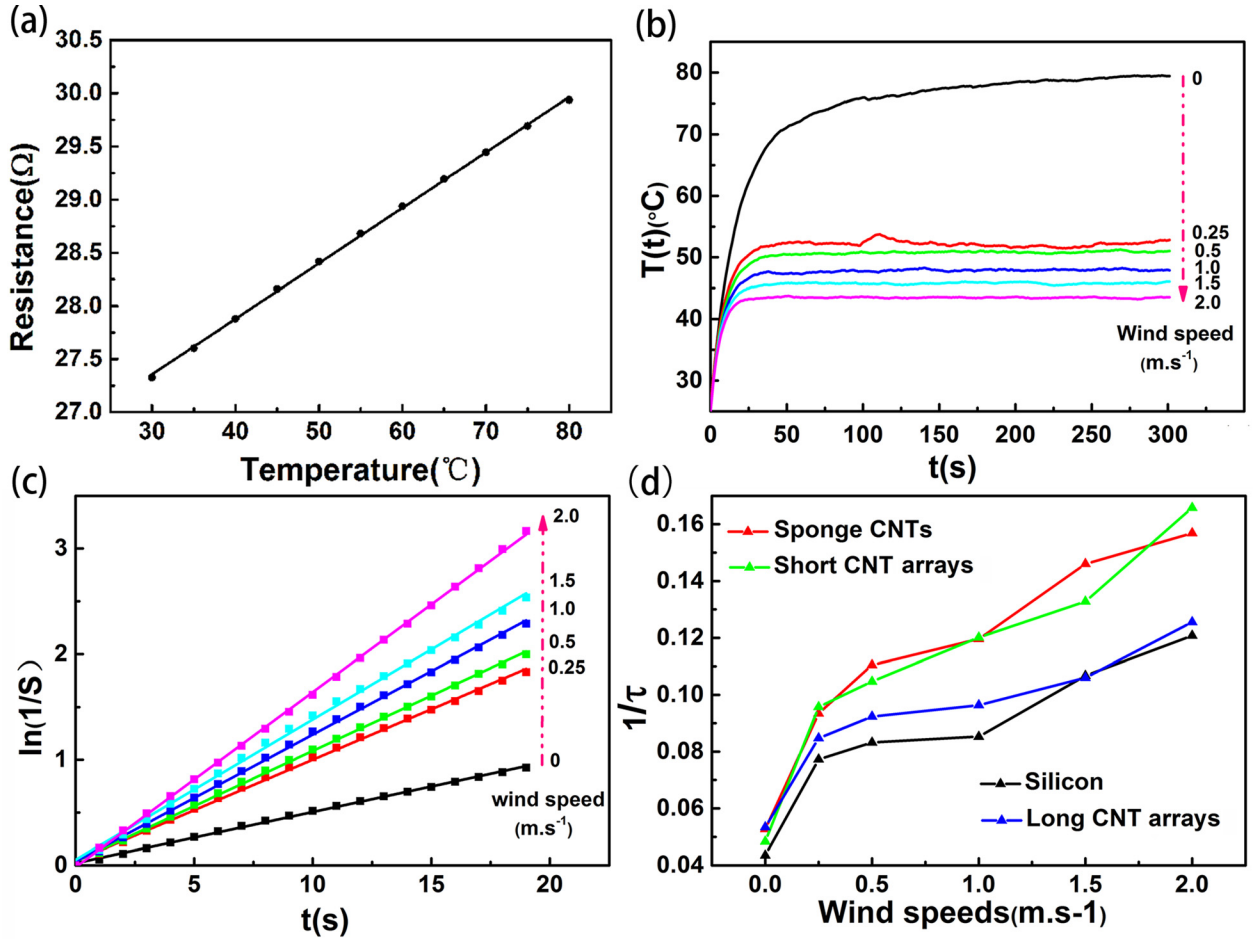

FIG. 3. (a) Heating electrodes' resistance at different temperature. (b) The temperatures of electrodes versus time after a current of 100 mA was applied. (c) The relationship between ln $\frac{1}{S}$ and time. The definition of S is shown in Eq. (4). Both (b) and (c) are tested on chips with short CNT arrays heat sink. (d) The values of $\frac{1}{\tau}$ versus the wind speeds for all four kinds of heat sink. The definition of $\frac{1}{\tau}$ is shown in Eq. (2).

$$T(t) = T(0) + \Delta T_{ss} \times (1 - e^{-t/\tau}), \tag{1}$$

$$\frac{1}{\tau} = \frac{hA}{mc}, \tag{2}$$

where $T(0)$ is room temperature, ΔT_{ss} is the difference between the balanced temperature and $T(0)$, m is the mass of the heat sink, c is the specific heat, h is the convection heat exchanging coefficient of heat sink, A is the area of heat sink contacted with air, and τ is an intrinsic parameter of heat sink, determined by Eq. (2).

Equation (1) can also be written as

$$\ln\left[\frac{1}{S}\right] = \frac{1}{\tau} \times t, \tag{3}$$

where

$$S = \left(1 - \frac{T(t) - T(0)}{\Delta T_{ss}}\right). \tag{4}$$

Fig. 3(c) shows ln $\left(\frac{1}{S}\right)$ versus t for short CNT arrays heat sink, with different wind speeds. It can be observed that for all the wind speeds, there is a linear relationship between ln $\left(\frac{1}{S}\right)$ and t. The values of the slopes at different wind speeds were obtained by fitting the data for all four kinds of heat sinks. Thus, the values of $\frac{1}{\tau}$ for different heat sinks and wind speeds can be determined and were plotted in Fig. 3(d).

As shown in Eq. (2), $\frac{1}{\tau}$ is determined by heat exchange coefficient h, area A, mass m, and specific heat c of the heat sink. For a certain heat sink, A, m, and c are constant and do not change with the wind speed. But the heat exchange coefficient h can be influenced by the wind, as reflected by the change of $\frac{1}{\tau}$ with the wind speed. As shown in Fig. 3(d), in circumstance with natural convection (wind speed = 0), the long CNT array's heat sink has the highest value of h with its largest surface area and the columnar structure. Compared with natural convection, the heat exchange coefficient for long CNT arrays heat sink increases by 58% with the wind speed of 0.25 m/s and the value increases by 98% at the wind speed of 1.5 m/s. With the increase of the wind speed, it is interesting to see that the heat exchange coefficients of sponge CNTs and short CNT arrays tend to be change even greater than that of the long CNT arrays. The heat exchange coefficient increases by 77% for sponge CNTs and 98% for short CNTs at the wind speed of 0.25 m/s. When wind speed reaches 1.5 m/s, the heat exchange coefficient of sponge CNTs and short CNTs increases by 177% and by 175%, respectively. These results imply that sponge CNTs and short CNT arrays are more sensitive to the wind speed than long CNT arrays. Sponge CNTs are porous and

have more interspaces among the branches, which make the gas flow passes though the sponge CNT heat sink more easily than CNT arrays. The CNT array is a dense and compact structure, which makes it resistive to lateral gas flow. However, short CNTs arrays, which are only 500 μm, can conduct more heat to the top than long arrays. That means gas flow on the top surface of the CNTs arrays can take away more energy than that around the side surface of the arrays, which makes short arrays sensitive to wind than the long arrays since the former has a higher ratio of top to side surface area.

When the heat dissipation comes to the steady stage, the temperature tends to be a balanced value T_b. We describe the thermal resistance θ of a heat sink by the following equations:

$$\theta = \frac{T_b - T_r}{P}, \tag{5}$$

$$\theta = \theta_{conduction} + \theta_{convection}, \tag{6}$$

$$\theta_{convection} = \frac{1}{hA}, \tag{7}$$

where T_b is the balanced temperature, T_r is the room temperature, P is the heating power, $\theta_{conduction}$ is the conduction thermal resistance which is decided by the thermal conductivity of materials and the interface thermal resistance, $\theta_{convection}$ is convection thermal resistance between the heat sink and air. Convection thermal resistance is decided by the area contacted with the air and the heat exchange coefficient h, as shown in Eq. (7). The heat exchange coefficient h can be influenced by the airflow velocity, so convection thermal resistance will change with the wind speed, whereas the conduction thermal resistance will not. Equation (5) can be rewritten as

$$T_b = \theta \times P + T_r. \tag{8}$$

From Eq. (8), it can be seen that T_b has a linear relation to P. Experimentally, the relationship between the balanced temperature T_b and the heating power P was measured for the four kinds of heat sinks, under the circumstance with different wind speeds. As the relationships are similar for all four types of the heat sinks, the result for the one with long CNT arrays is plotted in Fig. 4(a) as an example. The thermal resistances of the long CNT array heat sink can be determined from the slope of the plot. As shown in Fig. 4(a), the thermal resistance decreases with the wind speed, which can be ascribed to the change of the heat exchange coefficient h. This trend is also observed in the other three samples. The thermal resistances of the heat sinks at different wind speeds are shown in Table I. To have a visual understand of the cooling effect, using Eq. (8) and thermal resistances value shown in Table I, we calculate the balance temperature T_b at different wind speeds for all the four kinds of heat sink when the heating power is 0.25 W, as shown in Fig. 4(b). Under natural convection, the heat sink based on long CNT arrays has the best cooling effect and the balanced temperature is 61.3 °C, 19% lower than that of bare silicon (75.8 °C). Only 1.9% lower temperature is observed in the sponge CNTs, indicating it has the poorest cooling effect among the CNT

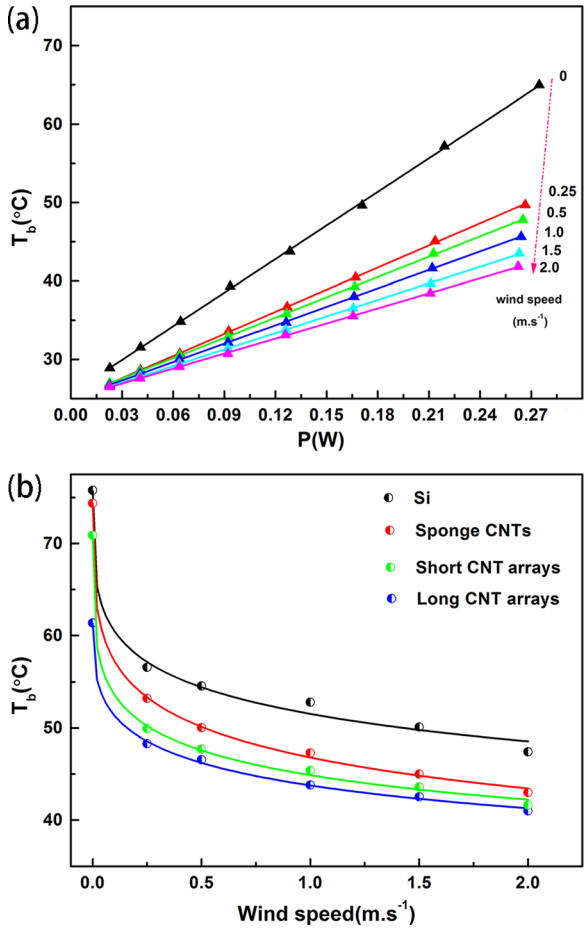

FIG. 4. (a) The balanced temperature versus the heating power at different wind speeds. (b) The balances temperature versus the wind speed for different kinds of heat sink.

based heat sink (6.2% and 19% lower temperature for short CNT array and long CNT array). Under the forced convection condition, balanced temperature for all kinds of heat sink has an obvious drop. When the wind speed is 2.0 m/s, the balanced temperature of sponge CNTs and short CNT array both decrease by about 40%, even more than those for the bare silicon and long CNT array (both of which decrease by about 35%). The results verify again that the sponge CNTs and the short CNT array are more sensitive to the airflow. CNT arrays have the same growth orientation and stand one by one. This structure is benefit for natural convection, because the heat from the underneath chip can be transferred to the top of CNT more conveniently in such a highly oriented structure. However, this kind of highly oriented structure is resistive for the lateral gas flow. Besides, from the

TABLE I. The thermal resistances (K/W) of the heat sinks at different wind speeds.

Heat sink type \ Wind speed (m/s)	0	0.25	0.5	1	1.5	2
Si	196.7	125.0	118.2	111.2	100.7	89.9
Sponge CNTs	195.9	113.7	100.4	90.4	80.1	71.5
Short CNT arrays	180.2	98.7	90.7	82.0	74.8	66.5
Long CNT arrays	142.9	94.0	86.2	78.4	70.3	63.9

Fig. 4(b), we can observe that long CNT arrays always have a better performance than the short CNT arrays, although they have the same structure. It is because the long CNT arrays are taller than the short CNT arrays, which makes larger contact area with air for the heat sink based on long CNT arrays. As shown in Eq. (7), the convection thermal resistance $\theta_{convection}$ is inversely proportional to the heat dissipation area. That means the long CNT arrays have smaller convection thermal resistance than the short CNT arrays. On the other hand, for CNTs heat sink, the main conduction thermal resistance $\theta_{conduction}$ is contributed by the interface between electronic device and CNTs. In our experiments, we used the silver paste with high thermal conductivity to bond the substrate with the heat sink (carbon nanotube arrays or sponge CNTs). For all the samples, the same dosage of the silver paste, the same solidify temperature, and the same solidify time have been used to minimize the variation in interfacial thermal conductivity among samples. Thus, the total thermal resistance θ ($\theta_{convection} + \theta_{conduction}$) of the long CNT arrays is smaller than that of the short. From Eq. (8), we know the balanced temperature is in direct proportion to the total thermal resistance. So the long CNTs have lower balanced temperature than the short, when the heating power and the room temperature are the same. Although the sponge CNTs have worse performance in natural convection condition compared to CNT arrays, this type of CNT is more sensitive to the wind speed and more suitable in the forced convection condition.

IV. CONCLUSIONS

In summary, the CNT's heat sink is very helpful for the heat dissipation of a micro heat source, according to the experiment results discussed above. However, depending on the different microstructures of the sponge CNTs, the short CNT array and the long CNT array, working conditions to achieve their best performance may vary. The long CNT array is a good choice for passive cooling for its high heat dissipation efficiency even under natural convection. But, the sponge CNTs show little benefit in heat dissipation if there is no airflow. On the other hands, the long CNT arrays are not necessary in the circumstance with a high speed air flow, since a short CNT array based heat sink which is more cost-effective shows even better performance. Besides, sponge CNTs are also a good choice if there is some airflow. Not only sponge CNTs can get the same heat dissipation effect in this conduction compared to the short CNT arrays but also the sponge CNTs based heat sink prone to assemble more easily due to its flocculent structure. The interconnected structure makes the sponge CNTs uneasy to fall off, which is very important for the stability of electric circuit. These results can provide a good reference for the choice of different CNTs as a chip heat sink at different conditions and it is very useful to promote the applications of CNT based heat sink, which is lighter, more efficient, and takes up less space compared to the traditional metallic heat sink.

ACKNOWLEDGMENTS

This work is supported by the National Basic Research Program of China (973 Program) under Grant No. 2015CB351905, the National Natural Science Foundation of China (No. 61306015), and Guangdong Innovative Research Team Program (No. 201001D0104713329).

[1]J. Klett, R. Hardy, E. Romine, C. Walls, and T. Burchell, Carbon **38**, 953 (2000).
[2]B. Lee, J. S. Lee, S. U. Kim, K. Kim, O. Kwon, S. Lee, J. H. Kim, and D. S. Lim, J. Vac. Sci. Technol. B **27**, 2408 (2009).
[3]A. A. Balandin, S. Ghosh, W. Bao, I. Calizo, D. Teweldebrhan, F. Miao, and C. N. Lau, Nano Lett. **8**, 902 (2008).
[4]S. Berber, Y.-K. Kwon, and D. Tomanek, Phys. Rev. Lett. **84**, 4613 (2000).
[5]T.-Y. Choi, D. Poulikakos, J. Tharian, and U. Sennhauser, Nano Lett. **6**, 1589 (2006).
[6]R. R. Bacsa, C. Laurent, A. Peigney, W. S. Bacsa, T. Vaugien, and A. Rousset, Chem. Phys. Lett. **323**, 566 (2000).
[7]A. Peigney, C. Laurent, E. Flahaut, R. R. Bacsa, and A. Rousset, Carbon **39**, 507 (2001).
[8]K. Kordás, G. Tóth, P. Moilanen, M. Kumpumäki, J. Vähäkangas, A. Uusimäki, R. Vajtai, and P. M. Ajayan, Appl. Phys. Lett. **90**, 123105 (2007).
[9]S. Jiang, C. Liu, and S. Fan, ACS Appl. Mater. Interfaces **6**, 3075 (2014).
[10]Y. Fu, N. Nabiollahi, T. Wang, S. Wang, Z. Hu, B. Carlberg, Y. Zhang, X. Wang, and J. Liu, Nanotechnology **23**, 045304 (2012).
[11]Q. Li, X. Zhang, R. F. DePaula, L. Zheng, Y. Zhao, L. Stan, T. G. Holesinger, P. N. Arendt, D. E. Peterson, and Y. T. Zhu, Adv. Mater. **18**, 3160 (2006).
[12]L. Li, K. Chen, L. Sun, S. Xie, and S. Lin, React. Funct. Polym. **73**, 83 (2013).
[13]J. Zhang, D. Jiang, and H.-X. Peng, Microporous Mesoporous Mater. **184**, 127 (2014).
[14]Z. Zeng, X. Gui, Z. Lin, L. Zhang, Y. Jia, A. Cao, Y. Zhu, R. Xiang, T. Wu, and Z. Tang, Adv. Mater. **25**, 1185 (2013).
[15]X. Li, A. Cao, Y. J. Jung, R. Vajtai, and P. M. Ajayan, Nano Lett. **5**, 1997 (2005).
[16]S. Talapatra, S. Kar, S. Pal, R. Vajtai, L. Ci, P. Victor, M. Shaijumon, S. Kaur, O. Nalamasu, and P. Ajayan, Nat. Nanotechnol. **1**, 112 (2006).
[17]S. A. Mirbagheri, A. Kazemzadeh, and A. A. Maghanaki, Jpn. J. Appl. Phys. Part 1 **51**, 015101 (2012).
[18]S. Liu, Y. Zhang, Y. Lin, Z. Zhao, and Q. Li, Carbon **69**, 247 (2014).